View metadata, citation and similar papers at core.ac.uk
brought to you by CORE
provided by Greenwich Academic Literature Archive

Allicin causes fragmentation of the peptidoglycan coat in *Staphylococcus aureus* by effecting synthesis and aiding hydrolysis: a determination by MALDI-TOF mass spectrometry on whole cells.

G.T.M Getti* and P.L.Poole
School of Health, Sport and Bioscience, University of East London, Water Lane, London E15 4LZ

* Correspondence address: Department of Life & Sport Sciences, Faculty of Engineering & Science, University of Greenwich, Chatham Maritime, ME7 3QY. Email G.t.m.getti@gre.ac.uk
Running headline: Induced autolysis of cell coat polysaccharides.

Abstract

Purpose: To determine the effect of allicin on *Staphylococcus aureus* cell wall peptidoglycans by the application of MALDI-TOF mass spectrometry on whole cells and to relate this to current knowledge of wall processing enzymes.

Methodology: Two different *S. aureus* strains were grown for 48 hours after which period each culture was split into two, one part was then treated with sub-inhibitory levels of allicin while the other part left untreated as a control. After a further 24 hours whole cells were recovered and analysed by MALDI-TOF mass spectrometry.

Results: Changes in the mass spectra between the treated and untreated cells revealed fragmented peptidoglycans identified by mass calculation only in the treated cells. These peptidoglycan fragments where identified as the products of specific peptidoglycan hydrolases.

Conclusions: Allicin is known to target cysteine thiol groups. These are absent in peptidoglycan hydrolases and we might had expected identical results in both of the treated and untreated cells. Peptidoglycan synthesis enzymes such as the Fem family of enzymes do contain cysteines. Fem enzymes A, B and X all have a conserved conformation of 99% of *S. aureus* strains in database and are therefore putative targets for allicin. Examination of FemA structure showed that cysteine102 is accessible from the surface. We propose that allicin has an inhibitory mechanism alongside others of targeting FemA and possibly other Fem enzymes by curtailing glycine

bridging and leading to fragmentation. This study provided an insight into yet another antimicrobial mechanism of allicin.

Key words

MALDI-TOF mass spectrometry, allicin, peptidoglycans, peptidoglycan hydrolases, Fem family of enzymes.

Introduction

The rapid spread of antibiotic-resistant pathogens poses a serious threat to public health. Gram-positive bacteria such as *S. aureus* are still giving concerns in the hospital environment and have become increasingly difficult to treat because of rapid development of resistant strains to common antibiotics. Penicillin resistant strains of *S. aureus* developed 4 years after the introduction of penicillin and have rapidly spread [1]. Similarly *S. aureus* strains resistant to methicillin (MRSA) developed 2 years after this drug was first introduced in Europe and are currently still recognized as a major problem in hospitals throughout the world [2].

Novel effective agents ideally with known mechanism of actions are needed. Allicin (Diallythiosulphinate, also known as Thio-2-propene-1-sulphinic acid S-allyl ester) from *Allium sativum* has been shown to exhibit anti-microbial properties to a number of microbes including reference strains and clinical isolates of *S. aureus.* Cutler and Wilson showed allicin to be active against cultured strains of methicillin resistant clinical isolates of 49 *S. aureus* at a minimum inhibitory concentration (MIC) of 16 μgxml^{-1} and to totally inhibit growth at 32 μgxml^{-1} [3]. As for methicillin-resistant clinical isolates obtained from the Royal London and St. Bartholomew's Hospitals, 30 were tested and 88% of those tested showed a minimum bactericidal concentration (MBC) of 128 μgxml^{-1} and were all killed at 256 μgxml^{-1}. The biological activity of allicin comes

from a reaction with thiol groups of cysteines to form S-allylmercaptocysteine as demonstrated in many proteins [4-7]. This is further confirmed by the fact that the antibacterial effect of allicin is abolished by cysteine, glutathione and coenzyme A in *S. aureus* and *E. coli* [8].

The cell wall of Gram-positive bacteria consist of polymers of thick layers of peptidoglycans comprises of N-acetylglucosamine (GlcNAc)→β1,4 N-acetylmuramic (MurNAc) disaccharides. MurNAc is linked to L-alanine through a lactyl side chain that then forms further linkages to other stem peptides that cross links to stabilize the structure. In *S. aureus* the next amino acid in the stem peptide is D-isoglutamine followed by L-lysine then by D-alanine. This last L-lysine forms a connection with its ε-amino group to the first glycine in a pentaglycyl bridge with the last glycine connecting to a neighbouring tetrapeptide alanine carboxyl group. There are a number of additions to these peptidoglycan layers principally that of wall teichoic acid (WTA) and O-acetylation.

We report the application of Matrix assisted laser desorption-ionization–time of flight mass spectrometry (MALDI-TOF mass spectrometry) carried out so to allow components of the cell coat to be analysed following cell disruption and release through a laser impacting the cell surface [9]. This is particular useful for the examination of the 'tough' cell wall of Gram-positive bacteria and is ideal for the analysis of small and large molecular mass components at or in the cell surface. We apply this analysis to untreated and allicin treated *S. aureus* cells. Results are interpreted by accessing the vast amount of documented molecular information in protein Data bases on *S. aureus* strains.

Methods

Allicin originally from Allicin International Limited (Half House, Military Road, Rye, East Sussex, UK) was kindly donated to us by Dr. Ron Cutler in a 5.0 $mgxml^{-1}$ solution in water. Allicin International had previously tested purity and confirmed concentration by HPLC. Further allicin verification was achieved by us with MALDI-TOF mass spectrometry. Allicin although containing two allyl chains is soluble in water up to 5.0 $mgxml^{-1}$. Allicin has been reported to be stable as measured by antibacterial activity towards *S. aureus* at 23ºC in aqueous solution with a half-life of about 6.5 days, while in a 20% ethanol solution it has a biological half-life of about 17.6 days and in 70% ethanol solution 8.7 days [10]. Allicin is unstable in hexane (half life of 8.8 hours) and vegetable oil (half life 2.4 hours). Because of the stability and maintenance of activity in an aqueous extraction this is the recommended procedure and organic extraction is avoided [3].

Bacteria Cultures

S. aureus strains: oxford (NCTC 6571) and a clinical isolate strain were donated by Dr Ron Cutler originally obtained from the Royal London and St. Bartholomew's Hospitals. These two strains were known to be inhibited by allicin. These two strains were grown as separate liquid cultures in Mueller-Hinton broth (Oxoid CM405) with gentle shaking at 37ºC. After 2 days of growth each culture was split into two and placed into two separate 50 ml centrifuge tubes. A final concentration of 63 $\mu gxml^{-1}$ of allicin (sub-inhibitory levels) was added to one half of both cultures while the second half was left untreated. All four samples were incubated for a further 24 hours with gentle shaking at 37ºC. Whole cells were then recovered by gentle centrifugation at 300 x g for 6 minutes forming a loose pellet to avoid disruption to the bacteria surface. Cells were extensively washed twice in 0.15 $moll^{-1}$ saline containing 0.02 $moll^{-1}$ Tris-HCl pH 7.4 to

remove growth medium and excess allicin. In a third and final wash the Tris-HCl was omitted from the saline solution.

MALDI-TOF Mass Spectrometry

Samples were prepared by adding an equal volume of the matrix solution, 14% (w/v) α-cyano-4-hydroxycinnamic acid (CHCA) in 70% (v/v) acetonitrile containing 0.015% (w/v) Trifluoroacetic acid (TFA) to all of the recovered whole cells. CHCA was chosen as it forms small homogenous crystals therefore surrounding cellular and cell wall components. Moreover as it is considered to be a 'hard' matrix it would impart a high energy captured from the laser excitation to cellular and cell coat components thus leading to disruption and desorption of these components. A total of 1.2 µl of all four samples were carefully placed into separate matrix pre-coated wells (1 µl of matrix previously dried down into the wells) in a MALDI plate. Triplicates were prepared for both treated and untreated samples and allowed to dry down at room temperature. Once dry, the MALDI plate was placed into an AXIMA (Shimadzu Scientific Instruments, Inc) CRF+ mass spectrometer equipped with a N_2 laser (λ337nm) and configured for positive mode. The laser power was set at 65 kV and the collected signal voltages were between that of 20 – 45 mV. After calibration using peptide standards (Sigma-Aldrich MALDI standards: P14R mass 1,532.8582 Da and Bradykinin fragment 756.3997 Da) the samples are then analysed. At least 100 laser shots were collected around each well and averaged with the AXIMA Smooth Gauss program. Allicin was verified by the drying down of a small quantity of the original allicin solution into a matrix prepared well and subjected to MALDI-TOF mass spectrometry. All recorded spectra are displayed as relative abundance against mass/charge (m/z) in the range 1000 m/z to 12000 m/z..

Protein Resource Data Bank applications and Data Analysis.

Protein sequences of peptidoglycan processing enzymes were accessed from the National Centre for Biotechnology Information (www.ncbi.nlm.nih.gov). All sequence alignments were carried out on line with the program BlastP using the Database: non-redundant protein sequences (nr) and by entering the query organism. Full protein crystallographic structures were accessed from the Research Collaboration for Structural Bioinformation Protein Data Bank (www.rcsb.org/pdb/home/home.do) and detailed examination of the structure was carried out on line using the NGL 3D Viewer application [11,12]. If full protein structures were not yet available in the RCSB Data Bank then cysteine positions within a protein sequence are analysed on line by accessing the protein resource of UniProtKB that is available in ExPASy Bioinformatics Resource Portal (www.expasy.org).

In interpreting the results the term Δ_y is defined as a single difference (in units of m/z) between a calculated mass from the chemical composition and an experimentally determined mass measurement or between two experimental mass measurements. A relative percent error was calculated as 100 x (Δ_y / calculated value of m/z). The term $|\Delta|_y$ is a set of all absolute differences in a Data set, for example a Data set might contain all the absolute values of Δ_y for one cell strain within a spectral range. Correlation coefficients (r), means and standard deviations (SD) were then calculated from all the Data within $|\Delta|_y$ by using Microsoft Excel.

Results

Verification of Allicin.

MALDI-TOF mass spectra of allicin is presented in Fig. 1 and demonstrates that on drying down in the matrix coated wells highly concentrated allicin aggregates are formed. No allicin mass peaks were found at around 162 m/z however between every consecutive aggregate peak there

was a mean difference of 162.17 m/z and this agrees well with the literature values of allicin (162.265 Da). Each peak has been assigned as an allicin aggregate plus trifluoroacetic acid (TFA^-) that was present in the matrix and confirmed with the formula $[n(162.17)/2 + (TFA^-)/2]^{2+}$ with values of n from 8 to 22 (in steps of 2) and 113.02 Da for TFA^-. This gave an overall mean with the Data set $|\Delta|_y$ between all the calculated and the recorded values of 0.11 m/z with a SD of 0.033 m/z. No other contaminant appeared too co-precipitated with the aggregates supporting the purity of the allicin.

Comparison of treated to untreated cells.

MALDI-TOF mass spectra showed a clear a difference between allicin treated *S. aureus* strains (Fig. 2 traces iv to vi) when compared with control untreated strains (Fig. 2 traces i to iii) in the mass range 1100 m/z – 2000 m/z for both of the two strains. In the oxford strain Fig. 2(a), there are also differences in the mass range 2000 m/z to 10000 m/z while in the cell strain Fig. 2(b), some similarity in the mass profile remains. This is a reflection of the fact that MALDI-tof profiles belong to two different strains attained from different biological sources (13).

A total of 18 major peaks with an average spacing of ~44 m/z were identified in the expanded view of the mass range 1100 m/z – 2000 m/z for both treated cell strains (Fig. 3). Between each peak ~18 minor peaks (~30 – 50% the intensity of the larger peaks) are present with an average spacing of ~44 m/z and shifted up from the larger peak by 15 – 16 m/z. These minor peaks also have their own satellite peaks. As these peaks are not found in the untreated cells we can exclude any extraneous attachment of agents arising from the culture medium or from a Matrix-induced fragmentation process or by pulse source decay (PSD).

A similar profile of peaks have been previously reported by MALDI-TOF spectrometry of different ratios and degrees of polymerisation (DP) of $(GlcN)_n$ and $(GlcNAc)_m$ and with chitin oligosaccharides (sodium and potassium adducts) with the majority of peaks in the range between 600 m/z – 3000 m/z [*14,15*]. Examination of our multiple peaks in the 1150 m/z – 2000 m/z region in the allicin treated cells showed a similar pattern, however our peaks did not extend much beyond 2000 m/z. The highest peaks are likely to arise from sodium adducts (+23) of saccharides as our cells were prepared from saline and these being one of the most commonly detected in MALDI mass spectrometry of saccharides. Boneca [*16*] obtained spectra for oligosaccharides extracted from *S. aureus* however, their results were obtained by PSD on a 3-aminoquinoline derivative (sodium adducts) rather than on cells directly. Therefore are not likely to reveal as much information on the processing and degradation of the cell wall compared to whole cell analysis. Our peaks arise from smaller oligosaccharide fragments from possible digestion of peptidoglycans or from fragmentation of the PIA or other cellular oligosaccharides but directly from whole bacteria unmodified samples and thus highly representative of the live cells state. These fragments were found only in the allicin treated cells after extensive washing suggesting that they must remain buried under or in the cell coat during growth and only released when undergoing MALDI-TOF spectrometry.

Gram-positive bacteria may be O-acetylated (OAc) at position C6 on MurNAc by one of the key cytoplasmic membrane enzyme O-acetyltransferase OatA [17, 18]. The spacing between our peaks is on average 44 m/z which can be explained by the degree of O-acetylation that may occur for Bacteria peptidoglycans. Although we would expect the spacing's to be 42 m/z the difference may reflect additional chemistry with the matrix. The most common reduction mechanism would be of a hydride reaction which is unlikely to take place in this instance as a strong hydride donor

is absent in our samples. We therefore propose the existence of two other possible reactions which could take place within the matrix:

i. Single electron stepwise reactions

$$R - O - CO - CH_3 + e^- \rightarrow [R - O - C^{e}O^{-} - CH_3] + H^+ \rightarrow [R - O - C^{e}OH - CH_3] + e^- \rightarrow$$
$$[R - O - C^{-}OH - CH_3] + H^+ \rightarrow R - O - CHOH - CH_3$$

ii. Enol tautomer reactions

$$R - O - CO - CH_3$$
$$\updownarrow$$
$$[R - O - COH = CH_2 \leftrightarrow R - O^{+} = COH - C^{-}H_2] + H^+ + 2e^- \rightarrow [R - O - C^{-}OH - CH_3] + H^+ \rightarrow$$
$$R - O - CHOH - CH_3$$

The single electron stepwise reaction requires a strong electron donator and could be facilitated by the production of free electron and protons which are passed on to the substrate following laser ionization of the matrix [9]. Secondly although esters are harder to reduce then aldehydes or ketones as they exist principally in an oxygen-bonded ketone, the enol tautomer is able to undertake an acid-catalysed reaction as the transient double bonded central carbanion is nucleophilic and is reactive to electrophiles such as the cationic H^+. Again we propose that this reaction may be aided by the laser ionization of the density packed matrix freeing up electrons and protons and passed on to the tautomer. Whichever reaction may take place a hemiacetal is rapidly generated. The solid phase of the matrix restricts movement of substrates and curtails any further addition reactions.

Assignments of fragments from peptidoglycans

To identify whether these fragments have arisen from the peptidoglycan layers it was necessary to examine peptidoglycan processing enzyme specificities as well as their products and susceptibility, if any, to allicin. Product assignment was achieved by the calculation of expected mass from peptidoglycan fragments. The value of 42.02 m/z was assigned to the N-acetyl group

for the non O-acetylated parent compound. Any additional O-acetylation carries a value of 44.02 m/z which is consistent with the near constant differences in most of the assigned masses. If differences between the calculated and measured mass in some of the assignments are considerably different than expected for mass spectra this might be attributed to some underlining peaks, drifting of the standardization or baseline variation. We therefore disregarded an assignment with differences greater than +/-1.5 m/z (average relative error of 0.10%) if found in both of the *S. aureus* strains.

Under normal circumstances the peptidoglycan layers in the cell wall undergoes digestion by hydrolases during septum cleavage, in the formation of pores in the cell wall and the releasing of turnover products during cell growth as well as autolysis when under shock conditions. There are several enzymes responsible for this hydrolysis [18]. One of the key enzymes is the peptidoglycan aminohydrolase that of N-acetylmuramoyl-L-alanine amidase. This enzyme cleaves the bonds between that of N-acetylmuramoyl→L-alanine and is located on the outer side of the cytoplasmic membrane and protruding into the narrow periplasmic space. Given the vast amount of information of allicin targeting cysteines thiol groups in many enzymes we undertook a search of the NCBI protein sequence Data Bank with the BlastP alignment program and choosing query proteins from *S. aureus* (Table 1). No cysteines likely to interfere with enzyme activity were found. Thus we propose that this enzyme is still active and able to cleave the stem peptide from the polysaccharide layers.

The exolytic transglycosylases such as the soluble lytic transglycosylases, hydrolyze β-1,4 glycosidic bonds between N-acetylmuramic acid→N-acetylglucosamine and generally located in the narrow periplasmic space. This enzyme generates an anhMurNAc terminal glycan. The lytic transglycosylases are inhibited by O-acetylation on MurNAc thus anhMurNAc(OAc) is not found

[20]. Given the mass range of between 1000 m/z to 2000 m/z, we calculated the position (assuming a charge of +1) of peaks in a mass spectra by summing the masses and taking into account loss of water as:

$$(\text{MurNAc GlcNAc})_n (\text{OAc})_y \text{ anhMurNAc} + 23 \text{ (for } Na^+ \text{)}$$

Where n is number of disaccharides, y is total number of $(OAc)_y$ groups.

Five corresponding masses (Table 2) that might be attributed to the enzyme products were found in our mass spectra in the mass range 1255 m/z to 1432 m/z with the number of disaccharides (n) of 2. Unfortunately no *S. aureus* soluble lytic transglycosylases (SLT's) have been sequenced. However other Bacillales and Lactobacillales SLT's enzyme sequences or domains have been sequenced and in Table 1 we present a survey of cysteines in fourteen SLT's that are to be found in the UniProtKB Data bank (several strains have multiple entries and we have avoided reproducing these in our list). There were no cysteines found in any of these SLT domains. Although this is not a conclusive survey it is indicative that *S. aureus* might also be free of any cysteines in the SLT domain, explaining the recording of these cleavage products.

Additional hydrolysis occurs with endo-β-N-Acetylglucosaminidase [*16*]. This enzyme will hydrolyse bonds between N-acetylglucosamine→N-acetylmuramic acid. We calculated the position (assuming a charge of +1) of the peaks in this region:

$$\text{MurNAc } (\text{GlcNAc MurNAc})_n \text{ GlcNAc } (\text{OAc})_y + 23$$

Table 2 presents some mass fragments that could be attributed to the enzyme products in the mass range 1475 m/z to 1741 m/z with the number of disaccharides (n) of two. A BlastP alignment of this enzyme revealed that there is no cysteine residues found in any of 71 matched enzymes entries (Table 1).

In the ranges 1387 m/z to 1432 m/z and 1651 m/z to 1741 m/z an unexpected addition of O-acetyl groups was needed to explain these assignments. We referred to this as Epi-acetylation. These results do suggest that some GlcNAc in addition to MurNAc are O-acetylated which has not been previously reported in *Staphylococcus* strains. As O-acetylation inhibits binding to some of the hydrolases discussed above, this further O-acetylation would occur after fragmentation of peptidoglycans. These shorter fragments are free from any rigid constraint within the peptidoglycan layer where they were previously attached and are now occupying the narrow periplasmic space thus coming in contact with the protruding catalytic domain of OatA. An increased flexibility of these fragments is achieved by the cleaving of the lactyl-alanine bond allowing rotation of the lactyl group on MurNAc with this lactyl side chain now able to take up different conformations as well as any rotational flexibility around the disaccharide β1-4 bond and presumably different spatial orientation of these smaller fragments. This could reduce any steric hindrance so the C6 hydroxyl of GlcNAc that may now enter the substrate binding site of OatA. Moreover these shorter fragments would become entangled in this narrow periplasmic space and this would explain why these fragments are only released on undergoing MALDI spectrometry and while not in the culture medium. Interestingly Sharif et al reported a partial thickness of the cross and outer cell wall at the septum as measured by TEM in Fem-deleted mutant *S. aureus* cells [21]. They suggested that this was likely formed by the accumulation of immature peptidoglycans in these Fem-deleted mutant cells. This agrees with our findings of peptidoglycan fragmentation.

As O-acetylation is dependent on the enzyme OatA, the inhibitory effect of allicin on this enzyme was explored. The enzyme is separated into two domains the N-terminal domain contains 11 closely packed transmembrane helices and two cysteines at positions 96 and 220 [22]. There are no transmembrane helices or cysteines found in the C-terminal domain. The C-terminal domain

protrudes out from the cytoplasm membrane into the narrow periplasmic space and carries the residues for a serine esterase activity. As these two domains are well separated it does place a distance from the activity region of the enzyme to those cysteines present in the N-terminal domain. Finally a BlastP run matched up >100 other *S. aureus* OatA entries (Table 1) with these two cysteines in the identical positions confirming a conserved conformation in these enzymes.

Although we have not been able to assign all of the mass spectra to oligosaccharides (fragmented or not) it is clear there are consistent differences between the spectra of allicin treated and untreated bacteria. Masses in the range between 2000 m/z – 10000 m/z are due to the presence of longer polymers, or other cellular components. Significantly the relative abundance of the majority of the mass peaks in the treated cells compared to the untreated cells has decreased in both cell strains as expected. This is particularly evident in the regions of 4200 m/z – 4400 m/z and that of ~6400 m/z and in the oxford strain at ~6800 m/z. Although loosely held surface polymers at the higher mass peaks might have been loss through the washing procedure the lack of such a loss on the control untreated cells suggests it is not. In addition in the treated oxford cell line some peaks showed increased intensity, in particular those at around 4823 m/z and 9529 m/z suggesting desorption of polymers of increased lengths or of new cellular components. These differences occurred consistently in all three independent prepared biological replicates confirming that they are representative of changes in the cell themselves.

Discussion

The analysis of the results showed consistency with previous reports. DP was calculated by adding to the lengths of the fragments found in the ranges 1250 m/z – 1432 m/z to the the GlcNAc end of those cleaved in the range 1475 m/z – 1740 m/z and proposes a minimal degree of polymerisation of 5 - 6 disaccharides with a loss of one GlcNAc to form a anhMurNAc terminal

end. This is in agreement with Boneca et al. who identified 3 - 10 disaccharides in *S. aureus* with an average of 5 - 6 and numbers of greater than 11 being present in low abundances [16]. Similarly, Dmitriev et al. derived by computer simulation the numbers of disaccharides in a peptidoglycan strand in *E. coli* [23]. They presented slightly higher results of between 4 - 30 disaccharides in numbers and peaking at 8 - 11 disaccharide units and falling off rapidly after this. As oligosaccharide minimal binding sites for hydrolases vary between 3 and 6 [19] with hydrolysis falling off rapidly after 5 – 6 oligosaccharides. It is therefore not surprising that we only obtained cleaved units of 5 to 6 oligosaccharides in length.

We suggest that peptidoglycan fragmentation shown during allicin treatment is caused by the action of cysteine-free hydrolases. As allicin is unable to inhibit such hydrolases then is it likely to facilitate activation and an accessibility of hydrolases to peptidoglycans. Because of its small size (162 Da) allicin can easily pass though the peptidoglycan layer which is between 20 – 100 nm in thickness with pores ranging in size between 5 – 50 nm and is readily permeable through cell membranes [24-26]. Cell wall processing enzymes are therefore some of the first to come in contact with allicin. We propose that allicin is targeting some of the cell wall synthesis enzymes leading to a weakening of the lower peptidoglycan layer and leading to a fragmentation process while the cells are still in the culture medium. This explanation is supported by the fact that the fragmentation is not found in the untreated control cells even though we might expect that some hydrolases could still be activated or are already active in these control cells. To explore this possibility, the presence of cysteine free thiols groups and their location in wall synthesis enzymes was investigated.

The peptidoglycan synthesis pathway in *S. aureus* has been well documented with the final stages of synthesis being that of:

Phospho-N-acetylmuramoyl-pentapeptide-transferase (MraY) → Lipid I intermediate → Undecaprenyldiphospho-muramoylpentapeptide-β-N-acetylglucosaminyltransferase (MurG) → Lipid II intermediate → FemX → FemA → FemB → (translocation to outer membrane) → Transglycosylases → Transpeptidases.

Most importantly FemX and FemA are critical for the building of the pentaglycyl bridge with FemX adding the first glycine to the lipid II intermediate followed by FemA adding two glycine's then by FemB adding the final two glycine's. The crystal structure and the protein sequence of FemA from *S. aureus* have been determined [27]. Sequence Data has been deposited in both the RCSB protein Data Bank and the NCBL Data Bank (Table 1) and shown to contain two cysteine residues 56 and 102. A BlastP was run of this entry against all *S. aureus* (including methicillin resistant) entries and found these two conserved cysteine residues in >100 matching enzymes entries. The enzyme structure of FemA has a large globular domain with these two cysteines approximately 12.6 Å apart within the subdomain that of 1A and are too far apart to form a disulphide bridge and therefore presenting free thiol groups. The protein feature view in 1LRZ shows residue 56 is in an ordered hydrophobic β strand region while residue 102 is in an ordered hydrophilic β turn region. Examination of the crystal structure revealed cysteine 102 is accessible through a cavity of approximate dimensions 6.8 Å x 4.5 Å wide at the protein surface with this cysteine at the floor of this cavity. As allicin is approximately the size of an apolar amino acid and on folding through hydrophobic interaction of the two allyl chains it could potentially enter or partial enter into this cavity and causing a disruption to the protein conformation.

In FemB two cysteine residues are found in the first 100 matching enzyme entries. The full sequence alignment of FemA and FemB suggested that there is some similarity in these proteins

with 39% sequence identity, however only 1 cysteine matched up that of residue 102 [27]. The other residue 351 is aligned to an ordered α helix region of FemA. By measuring the distance from residue 353 which in FemA is an alanine (note. sequence numbering is increased by 2 for this cysteine position in 1LRZ) to cysteine 102 it is approximately 37.5 Å away and if both were now cysteines they could not form a disulphide bridge. Both of these cysteines will thus present free thiol groups. Interestingly this residue 102 is the cysteine that is accessible in FemA while residue 353 is closer to the L-shaped peptide binding pocket as well as to the protein outer surface. However it is most likely there are small differences in these two protein conformations so as to compare these two enzymes a full crystal structure of FemB would be required. In FemX only one cysteine residue 70 is found in >100 matching enzymes entries. The full sequence alignment of FemA with FemX again suggested some similarity (26% sequence identity) [27]. The Fem X cysteine did not match up with any cysteines in FemA. The position of cysteine 70 is found to be in an ordered β strand region of FemA. By superimposing onto the position of phenylalanine 70 in FemA it was found to lay in subdomain 1A and would have been close to position 102 which in FemX is now an alanine. However here again FemX might have a different conformation to FemA and we are not able to comment on the cysteine accessibility however this single cysteine must present a free thiol group.

Sharif et al [21] reported peptidoglycan fragmentation in *S. aureus* with Fem-deleted mutants also containing truncated pentaglycine bridging. Specifically with FemX-deleted mutants glycine bridging was absent. While in FemA-deleted mutants they found those with a single bridging glycine, cross-linking was decreased by ~20% leading to a high concentration of open N-terminus monoglycyl segments. Recently Kim et al [28] reported the architecture of peptidoglycans in wild type *S. aureus* and favoured that the peptidoglycan chains forms a vertical scaffold type model [*23*] perpendicular to the membrane with parallel orientation of the stem peptides. Kim suggested this is formed as the average number of disaccharide units is only 6 (also refer to our results

above) with the numbers of glycine's in the bridge being key factors in determining the types of different peptidoglycan architectures. Moreover they concluded there would be stem peptide 'crowding' when forming short bridges and presumably open gap segments between those stem peptides when a bridge is not formed. Applying this same reasoning to the proposed inactivation of FemA by allicin and a possible inactivation of other Fem enzymes, we should therefore expect to find open gap segments between stem peptides and an accumulation of immature peptidoglycans.

Finally we examined if any other peptidoglycan enzymes in *S. aureus* that might be affected by allicin and completed a search on key peptidoglycan enzymes in this later stage of synthesis. One cysteine residue was found in Phospho-N-acetylmuramoyl-pentapeptide-transferase (MraY) and again a BlastP run revealed the presence of one cysteine residue in all 80 matching enzymes. This cysteine is found to be in a long hydrophobic sequence and predicted using the resource UniProtKB with accession number entry Q2FZ93 to be in a transmembrane helix and buried within the cell membrane and therefore less accessible. No cysteine residues were found in Undecaprenyldiphospho-muramoylpentapeptide-β-N-acetylglucosaminyltransferase (MurG) or any of other 100 matching entries and with Transpeptidases (three PBP's). Finally the structure of a *S. aureus* Transglycosylase is deposited in the RCSB protein data base under 3VMQ. Running the sequence in BlastP revealed at least 23 excellent matches in which none of these contained cysteine. All these searches are summarized in Table 1.

Many of the enzymes explored that are involved in cleavage of peptidoglycans, do not have cysteines and therefore unlikely to be a target for allicin. The fragments identified here appear to be the products of some of the enzymes discussed. Daniels et al proposed there is a general exclusion of cysteines and disulphide bond formation in Firmicutes such as *S. aureus* [28]. This

agrees with the findings of these wall processing enzymes and in particular the hydrolases. Although we could not absolutely connect the effect of allicin with the peptidoglycan synthesis enzymes discussed above, these synthesis enzymes are likely to be affected as some do contain free cysteine thiol groups. The disruption of these peptidoglycan synthesis enzymes that contain free cysteines would potentially lead to a halting of any new or the ideal peptidoglycan structure. The most likely candidates as a putative targets for allicin are those free cysteines (and thus presenting thiol groups) that are found in the *S. aureus* FemXAB protein family of enzymes thus disrupting the assembling of the pentaglycine bridge formation. Furthermore, we are confident that these enzymes would be targets in other *S. aureus* strains as high identity matches (>99%) for the same Fem enzyme (FemA, B or X) suggest a conserved protein conformation with an identical arrangement of cysteines. This would also explain the wide inhibitory effect of allicin in *S. aureus* strains.

Taken together our results not only confirm that allicin is active against Gram-positive bacteria but indicate the existence of yet another mechanism of action. Allicin targets Fem enzymes causing gaps in the lower cell wall and facilitates hydrolases access to and fragmentation of peptidoglycans. Allicin ability to affect the cell wall makes it an ideal combination treatment with alcohol containing bactericides as it is likely to have a synergistic action on treatments as well as reducing the risk of a spread of antibiotic resistance.

Funding Information

This work received no specific grant from any funding agency.

Acknowledgements

We would like to thank Dr. Ron Cutler (School of Biological and Clinical Sciences, Queen Mary University of London) for his kind donation of allicin and the two *S. aureus* cell lines. MALDI-TOF was undertaken at the School of Health, Sport and Bioscience at the University of East London.

Conflict of Interest

There are no conflict of interest.

Ethical Statement

No human subjects or animals were used in these experiments.

References

1. **Chambers H.F.** The changing epidemiology of *Staphylococcus aureus*? Emerg Infect Dis 2001;7:178-182
2. **Palavecino E.,** (2004). Community-acquired methicillin-resistant *Staphylococcus aureus* infections. Clin Lab Med 2004; 24: 403-418
3. **Cutler R.R. and Wilson P.** Antibacteria activity of a new stable aqueous extract of allicin against methicillin-resistant Staphylococcus aureus. British Journal of Biomedical Science 2004; 61(2): 1-4.
4. **Ankri S., Miron T., Rabinkov A., Wilchek M. and Mirelman D.,** (1997). Allicin from garlic strongly inhibits cysteine proteinases and cytopathic effects of Entamoeba histolytica. Antimicrob Agents Chemother 1997; 41(10): 2286 – 2288.

5. **Rabinkov A., Miron T., Mirelman D., Wilchek M., Glozman S., Yavin E. and Welner L.** S-Allylmercaptoglutathione: the reaction product of allicin with glutathione possesses SH-modifying and antioxidant properties. Biochemica Biophysical Acta 2000; 1499(1-2): 144-153.

6. **Cruz-Villalon G. and Perez-Giraldo C.** Effect of allicin on the production of polysaccharide intercellular adhesion in Staphylococcus epidermidis. Journal Appl Microbiol 2011; 110(3): 723-728.

7. **Muller A., Eller J., Albrecht F., Prochnow P., Kuhlmann K., Bandow J.E., Slusarenko A.J., and Leichert L.I.O.** Allicin Induces Thiol Stress in Bacteria through S-Allylmercapto Modification of Protein Cysteines. Journal of Biological Chemistry 2016; 291(22): 11477-11490.

8. **Fuiisawa H., Watanabe K., Suma K., Origuchi K., Matsufuji H., Seki T. and Ariga T.** Antibacterial potential of garlic-derived allicin and its cancellation by sulfhydryl compounds. Biosci Biotechnol Biochem 2009; 73(9): 1948-1955.

9. **Clark A.E., Kaleta E.J., Arora A. and Wolk D.M.** Matrix-Assisted Laser Desorption Ionization-Time of Flight Mass Spectrometry: a Fundamental Shift in Routine Practice of Clinical Microbiology. Clinical Microbiology Reviews 2013; 26(3): 547-603.

10. **Fuiisawa H., Suma K., Origuchi K., Kumagai H., Seki T. and Ariga T**. Biological and chemical stability of garlic-derived allicin. Journal of Agricultural and Food Chemistry. 2008; 56(11): 4229-4235.

11. **Rose A.S. and Hildebrand P.W.** NGL Viewer: a web application for molecular visualization. Nucl Acids Res 2015; 43 (W1): W576-W579

12. **Rose A.S., Bradley A.R., Valasatava Y, Duarte J.M., Prlić A. and Rose P.W**. Web-based molecular graphics for large complexes. ACM Proceedings of the 21st International Conference on Web3D Technology (Web3D '16); 2016: 185-186,

13. **Singhal N., Kumar M., Kanaujia P.K., Virdi J.S.** MALDI-TOF mass spectrometry: An emerging technology for microbial identification and diagnosis. Front. Microbiol. 2015;6:791.

14. C**abrera J. C. and Cutsem P.V.** Preparation of chitooligosaccharides with degree of polymerization higher than 6 by acid or enzymatic degradation of chitosan. Biochemical Engineering Journal 2005; 25: 165-172.

15. **Chen M., Zhu X., Li Z., Guo X. and Ling P.** Application of matrix-assisted laser desorption/ionization time-of-flight mass spectrometry (MALDI-TOF-MS) in preparation of chitosan oligosaccharides (COS) with degree of polymerization (DP) 5–12 containing well-distributed acetylgroups. International Journal of Mass Spectroscopy 2010; 290: 94-99.

16. **Boneca I.G., Huang Z. H., Gage D.A. and Tomasz A.** Characterization of Staphylococcus aureus Cell Wall Glycan Strands, Evidence for a new β-N-Acetylglucosaminidase Activity. J Biol Chem 2000; 275: 9910-9918.

17. **Bera A., Herbert S., Jakob A., Vollmer W. and Gotz F.** Why are pathogenic staphylococci so lysozyme resistant? The peptidoglycan O-acetyltransferase OatA is the major determinant for lysozyme resistance of Staphylococcus aureus. Molecular Microbiology 2005; 55(3): 778 – 787.

18. **Bera A.,Biswas R., Herbert S. and Gotz F.** The Presence of Peptidoglycan O-Acetyltransferase in Various Staphylococcal Species Correlates with Lysozyme Resistance and Pathogenicity. Infection and Immunity 2006; 74(8): 4598-4604.

19. **Vollmer W., Joris B., Charlier P. and Foster S.** Bacterial peptidoglycan (murein) hydrolases. FEMS Microbiol Rev 2008; 32: 259-286.

20. **Weadge J.T., Pfeffer J.M. and Clarke A.** Identification of a new family of enzymes with potential O-acetylpeptidoglycan esterase activity in both Gram-positive and Gram-negative bacteria. BMA Microbiology 2005; 5:49.

21. **Sharif S., Sung Joon Kim, Labischinski H. and Schaefer.** Characterization of Peptidoglycan in Fem-deleted Mutants of Methicillin-resistant Staphylococcus aureus by Solid-State NMR. Biochemistry 2009; 48(14): 3100-3108

22. **Bernard E., Rolain T., Courtin P., Guilot A., Langella P., Hols P. and Chapot-Chartier M-P.** Characterization of O-Acetylation of N-Acetylglucosamine: a novel structural variation of Bacterial Peptidoglycan. J. Biol Chem 2011; 286; 23950-23958.

23. **Dmitriev B.A., Touach F.V., Schaper K-J., Holst O., Rietschel E. T. and Ehlers S.** Tertiary Structure of Bacterial Murein: the Scaffold Model. Journal of Bacteriology 2003; 185(11): 3458-3458.

24. **Touhami A., Jericho M.H. and Beveridge T.J.** Atomic Force Microscopy of Cell Growth and Division in Staphylococcus aureus. Journal of Bacteriol 2004; 186(11): 3286-3295.

25. **Meroueh S.O., Bencze KZ., Hesek D., Lee M., Fisher J.F., Stemmler T.L. and Mobashery S.** Three-dimensional structure of the bacterial cell wall peptidoglycan. PNAS 2006; 103(12): 4404-4409.

26. **Miron T., Rabinkov A., Mirelman D., Wilchek M. and Weiner L.** The mode of action of allicin: its ready permeability through phospholipid membranes may contribute to its biological activity. Biochimica et Biophysica Acta – Biomembranes 2000; 1463(1): 20-30.

27. **Benson T. E[1], Prince D. , Mutchler V. , Curry K. A, Ho A. M, Sarver R. W, Hagadorn JC, Choi G. H, and Garlick R. L.** X-ray crystal structure of Staphylococcus aureus FemA. Structure 2002; 10(8): 1107-15.

28. **Daniels R., Mellroth P., Bernsel A., Neiers F., Normark S., von-Heijne G. and Heriques-Normark B.** Disuphide bond formation and cysteine exclusion in Gram-positive Bacteria. J. Biol Chem 2010; 285(5) 3300-3309.

Table 1. Cysteines in Peptidoglycan Processing Enzymes: *Staphylococcus aureus* and SLTases in Firmicutes.

Enzyme	Query*	Matches	Cover	Identities	Cysteines
N-Acetylmuram**oy**l-L-Alanine Amidase	EWN33417	100	96-100%	99-100%	0
N-Acetylmuramoyl-L-Alanine Amidase (Amidase region (181 – 362) and includes the active site of this enzyme).	AID38810	100	98-100%	96-100%	
Soluble Lytic Transglycosylase (UniProtKB).	common Firmicutes†				0
Peptidoglycan endo-β-N-Acetylglucosaminidase	SAZ48439	71	98-100%	99-100%	0
Fem A	BAU34893	>100	100%	99-100%	2
Fem A (RCSB)	1LRZ	self			
Fem B	ADD85346	>100	100%	97-100%	2
Fem X	ADD85351	>100	100%	99-100%	1
MraY (UniProtKB)	Q2FZ93	self			1
MraY	BBA23731	80	100%	98-100%	
MurG	BAU34936	>100	100%	99-100%	0
Peptidoglycan Transpeptidase. (with region of PBP 2 and FtsI)	CEH26378	> 100	100%	99- 100%	0
D,D-Transpeptidase matches (UniProtKB) (identity match of >99% with region of *S. aureus* PBP 1 and FtsI)	A0A0E0VN59	34	100%	96-100%	0
PBP 2a (mrsa) (with FtsI region)	AKE50921	> 100	100%	99-100%	0
PBP 3 (99% match with PBP 2)	ANW82086	> 100	100%	99-100%	0
Peptidoglycan Glycosyltransferase (RCSB)	3VMQ	self			0
Peptidoglycan Glycosyltransferase.	EFC07480	23	100%	99-100%	
OatA	BAX76438	>100	100%	99-100%	2

* This is the NCBL accession query code (another DATA base). If sequences have shown to overlap, a partial sequence or has a low identity match a check has been made that those matched sequences do not contain cysteine. A few of the matches were with *Staphylococcus* multispecies.

† Firmicutes surveyed are *Bacillus*.strains: *subtills* (L8AQA9), *cereus* (A0A1Y6AXS), *anthracis* (D8H8F5), *thuringiensis* (A0A1C4C8S3), *megaterium* (A0A0H4R7E0), *mycoides* (A0A1G4EI40), *cytotoxicus* (A0A1D3QNU2); *Halobacillus.karajensis* (A0A024P953), *Listeria.monocytogenes* (A0A0E0UTJ9); *Lactobacillales/Streptococcus* strains: *pneumonia* (A0A0Y0B8K7), *anginosus* (F5U3V7), *suis* (A4VUN1); *lactis* (A0A0A7SYA5), *plantarum* (A0A165VKK5).

Table 2 Putative (best fit) of Oligosaccharide Fragments. Mass range 1255mz -1741m/z. Sodium adducts (major peaks only).

	Calculated m/z* A	B†	oxford m/z	102 m/z	Δ_{oxf} A	Δ_{102} A	Δ_{oxf} B	Δ_1 B	oxford % relative errors	102
$(MurNAcGlcNAc)_2$ anhMurNAc†	1255.27	1257.27	1255.27	1255.93	0	-0.66	2.00	1.34	0.000	-0.052
$(MurNAcGlcNAc)_2$ (OAc) anhMurNAc	1297.29	1299.29	1299.30	1299.90	-2.01	-2.61	-0.01	-0.61	- 0.001	-0.047
$(MurNAcGlcNAc)_2$ $(OAc)_2$ anhMurNAc	1339.31	1343.39	1343.48	1343.80	-4.17	-4.49	-0.09	-0.41	-0.007	-0.031
Epi-acetylation fragments										
$(MurNAcGlcNAc)_2$ $(OAc)_3$ anhMurNAc	1383.33	1387.33	1387.33	1387.84	-4.00	-4.51	0.00	- 0.51	0.000	-0.037
$(MurNAcGlcNAc)_2$ $(OAc)_4$ anhMurNAc	1425.35	1431.35	1431.33	1431.82	-5.98	-6.47	0.02	- 0.47	0.001	-0.033
$MurNAc(GlcNAcMurNAc)_2GlcNAc$†	1476.53	1478.53	1475.33	1475.84	1.20	0.69	3.20	2.69	0.081	0.047
$MurNAc(GlcNAcMurNAc)_2GlcNAc$ (OAc)	1518. 55	1520.55	1519.44	1519.91	-0.89	-1.36	1.11	0.64	0.073	0.042
$MurNAc(GlcNAcMurNAc)_2GlcNAc$ $(OAc)_2$	1560.57	1564.57	1563.46	1563.93	-2.89	-3.36	1.11	0.64	0.071	0.041
$MurNAc(GlcNAcMurNAc)_2GlcNAc$ $(OAc)_3$	1602.59	1608.59	1607.59	1608.01	-5.00	-5.42	1.00	0.58	0.062	0.036
Epi-acetylation fragments										
$MurNAc(GlcNAcMurNAc)_2GlcNAc$ $(OAc)_4$	1644.61	1652.61	1651.72	1652.09	-7.11	-7.48	0.95	0.52	0.057	0.031
$MurNAc(GlcNAcMurNAc)_2GlcNAc$ $(OAc)_5$	1686.63	1696.63	1695.54	1696.06	-8.91	-9.43	1.09	0.57	0.064	0.033
$MurNAc(GlcNAcMurNAc)_2GlcNAc$ $(OAc)_6$	1728.65	1740.65	1739.36	1740.02	-10.71	-11.37	1.29	0.63	0.074	0.036

* Masses in Daltons are taken as: GlcNAc 203.24 ($-H_2O$), MurNAc 293.27 ($+H_2O$), anhMurNAc 275.25 ($+H_2O$), GlcN 179. 17 ($+H_2O$), OAc 42.02 ($-H_2O$).

Example calculation for $MurNAc(GlcNAcMurNAc)_2GlcNAc$: 293.27 – 18 +(203.24 + 293.27) – 18 + (203.24 + 293.27) + 203.24 + 23 = 1476.53 m/z.

† Column A calculated mass, column B calculated mass increased by 2.0 m/z, refer to mass increase for carbonyl reduction (O-acetyl only) in text. Fragments marked † are calculated from values in column A (thus not increased by 2.0 m/z) these may act as internal standards.

Correlation coefficients r = 0.999 is recorded for $|\Delta|$ between both sets of experimental results and for the $|\Delta|$ calculated v for oxford and the $|\Delta|$ calculated v 102 experimental results.

Mean + SD for all results: $|\Delta|$ both measured experimental 0.50 + 0.10 m/z and calculated v experimental $|\Delta|_{oxford}$ 0.65 + 0.54 m/z, $|\Delta|_{102}$ 0.58 + 0.08 .m/z

FIGURE LEGENDS

Figure 1. MALDI spectrum recorded of pure allicin. Allicin forms progressive aggregates when drying down in the matrix prepared wells. This is most likely due to the hydrophobic nature of the folded allyl chains. The differences in the 5 peaks from 1029.39 m/z to 1840.27 m/z are: 162.18; 162.17; 162.16; 162.18; 162.18. Mean + SD = 162.17 + 0.009 m/z. This demonstrates the consistency throughout this region.

Figure 2. MALDI mass spectra recorded as in methods. (a) is the *Staphylococcus aureus* oxford strain, (b) is the 102 strain. In both of the mass spectra the top three spectra show those cells that have been treated with 63 $\mu g x ml^{-1}$ of allicin for 24 hour while the bottom three spectra are the untreated controls.

Figure 3. MALDI mass spectra. Expanded region 1100m/z – 2000 m/z of the treated two strains: top trace is oxford and bottom trace is 102. The values of {r} are a measure of the mass resolution.

Figure 1.

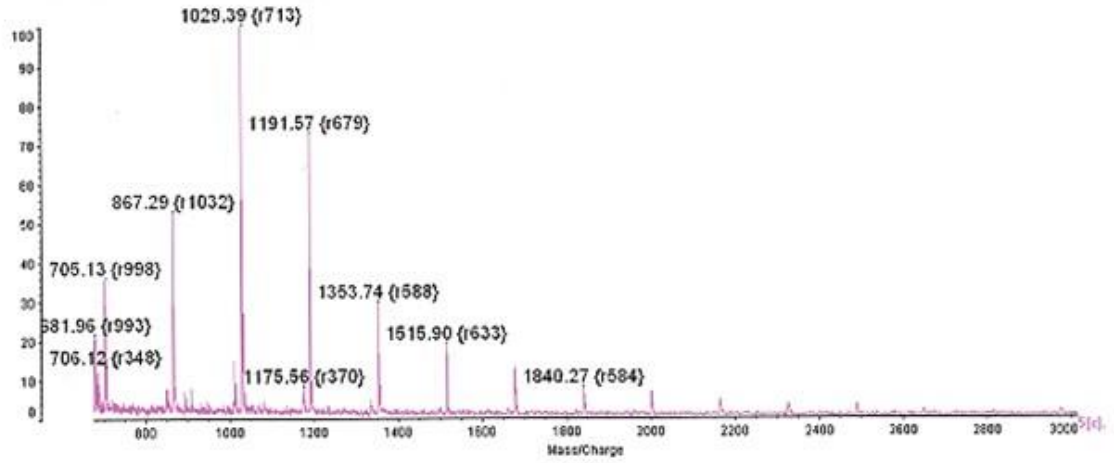
1029.39 (r713)
1191.57 (r679)
867.29 (r1032)
705.13 (r998)
1353.74 (r588)
581.96 (r993)
1515.90 (r633)
706.12 (r348)
1175.56 (r370)
1840.27 (r584)
Mass/Charge

Figure 2.

(a)

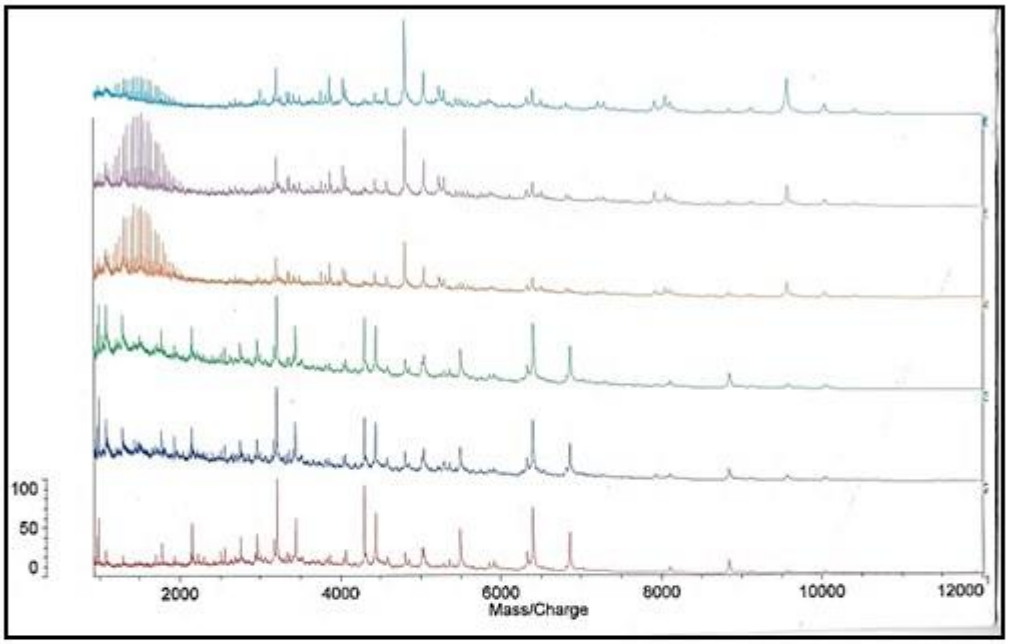
100
50
0
2000
4000
6000
8000
10000
12000
Mass/Charge

(b)

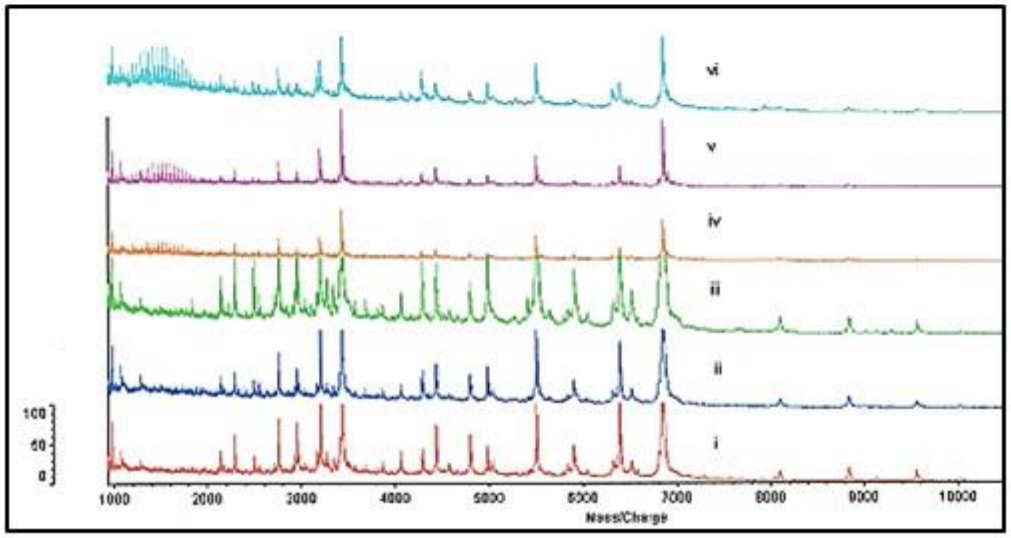
vi
v
iv
iii
ii
i
100
50
0
1000
2000
3000
4000
5000
6000
7000
8000
9000
10000
Mass/Charge

Figure 3.

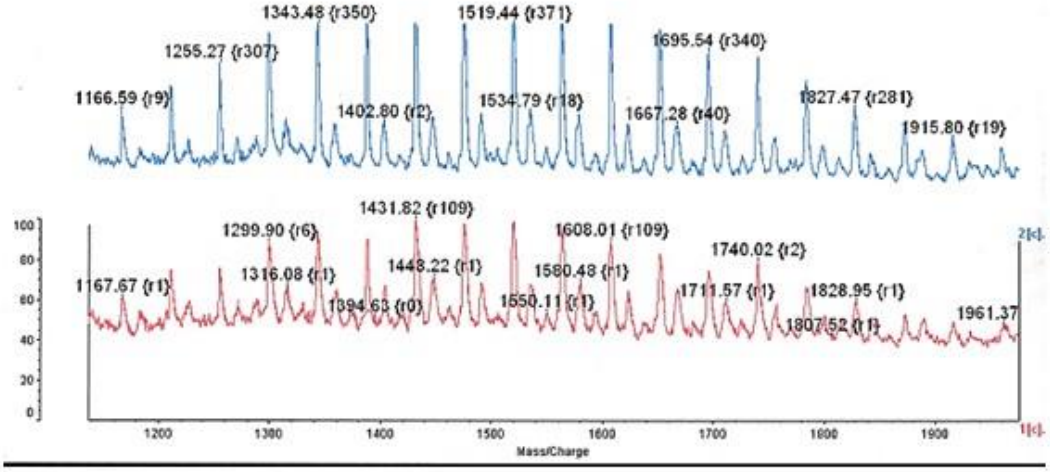
1343.48 {r350}
1519.44 {r371}
1255.27 {r307}
1695.54 {r340}
1166.59 {r9}
1402.80 {r2}
1534.79 {r18}
1667.28 {r40}
1827.47 {r281}
1915.80 {r19}
1431.82 {r109}
1299.90 {r6}
1608.01 {r109}
1740.02 {r2}
1316.08 {r1}
1448.22 {r1}
1580.48 {r1}
1167.67 {r1}
1711.57 {r1}
1828.95 {r1}
1394.63 {r0}
1550.11 {r1}
1807.52 {r1}
1961.37
100
80
60
40
20
0
1200
1300
1400
1500
1600
1700
1800
1900
Mass/Charge